Tetrahedron 67 (2011) 228–235

Contents lists available at ScienceDirect

Tetrahedron

journal homepage: www.elsevier.com/locate/tet

Synthesis of new porphyrin/fullerene supramolecular assemblies: a spectroscopic and electrochemical investigation of their coordination equilibrium in solution

Leandro J. Santos [a,*], Dayse CarvalhoDa-Silva [b], Júlio S. Rebouças [c], Marcos R.A. Alves [b], Ynara M. Idemori [b], Tulio Matencio [b], Rossimiriam P. Freitas [b], Rosemeire B. Alves [b]

[a] Universidade Federal de Viçosa—Campus de Florestal, Rodovia LMG, 818-km 6, Florestal—MG, CEP: 35690-000, s/n, Minas Gerais, Brazil
[b] Departamento de Química—Instituto de Ciências Exatas, Universidade Federal de Minas Gerais, Avenida Antônio Carlos 6627, Belo Horizonte—MG, CEP: 31270-901, Brazil
[c] Departamento de Química—Centro de Ciências Exatas e da Natureza, Universidade Federal da Paraíba, Campus I, João Pessoa—PB, CEP: 58059-900, CP: 5093, Brazil

ARTICLE INFO

Article history:
Received 12 August 2010
Received in revised form 17 October 2010
Accepted 22 October 2010
Available online 29 October 2010

Keywords:
Supramolecular complex
Zn-porphyrin
Fullerene-C_{60}
SQUAD

ABSTRACT

Two new fullerene ligands have been designed to provide relatively simple frameworks to build supramolecular systems containing both fullerene and Zn-porphyrin moieties. The coordination of the fullerene ligands to the Zn-porphyrin was supported by UV–vis titration, nuclear magnetic resonance and electrochemical data. The resulting spectrophotometric data were processed both graphically and computationally to yield the stoichiometry, stability constant, and molar absorptivity of the species in equilibrium.

1. Introduction

Porphyrin/fullerene systems and dyads have been extensively studied to examine donor/acceptor interactions.[1,2] Donor/acceptor interactions within fullerene/porphyrin assemblies are important for the design of multi-component model systems for photoactive materials[3] and light-harvesting devices.[4] Thus, chemists have increasingly sought to develop relatively simple donor/acceptor systems. Since Liddell and co-workers[5] reported the first synthesis of a C_{60} derivative covalently linked to a porphyrin, various other fullerene/porphyrin dyads have been synthesized based on covalently linked components.[6,7] Another attractive route to prepare such supramolecular assemblies has been the coordination of appropriately functionalized fullerene derivatives to metalloporphyrins, such as those containing zinc[8,9] or magnesium[10] as the metal center. In the latter route, the fullerene has often been functionalized with an *N*-heteroaromatic moiety. This metal/ligand coordination strategy provides a simple and versatile way to construct electron donor/acceptor assemblies, which may be of interest as mimics of the efficient biological electron transfer systems.[7]

With respect to the synthetic aspects, most of the fullerene ligands reported to date have been prepared by the functionalization of C_{60} in various steps in low-to-moderate yields. The prevailing strategy for the synthesis of fullerene ligands is via cycloaddition reactions.[11,12] For example, D'Souza and co-workers have synthesized fullerene ligands via [3+2] cycloadditions of azomethine ylides and C_{60}.[13,14] More recently, Deye and co-workers have designed a new ligand based on the Diels–Alder functionalization of C_{60}.[15] A less frequently used method to obtain fullerene ligands employs the Bingel's cyclopropanation reaction, which consists of the reaction of active methylene compounds with C_{60}.[16,17] The search for new fullerene/porphyrin supramolecular systems prompted us to design new functionalized fullerene ligands via the Bingel–Hirsch cyclopropanation of C_{60} and to evaluate the ability of these new ligands to assemble with a simple Zn-porphyrin, 5,10,15,20-tetraphenylporphyrinatozinc(II) (Zn(TPP)).

The accurate determination of the equilibrium constants (K) associated with dyad formation is often required in various chemical, biochemical, and pharmaceutical settings. In previous work, such constants for fullerene/porphyrin interactions have been determined by ^{1}H NMR,[18] UV–vis,[8,10,13,14,16,17,19] and fluorescence[9,10,17,18,21] spectroscopies. Whereas spectrophotometry has been the method of choice due to its simplicity, low cost, ease of adaptation, and high sensitivity (which allows the use of concentrations as low as 10^{-6} mol L^{-1}), it has also been limited to systems with minimal chromophore absorbance overlap.

In this contribution, we utilize a multiwavelength, multiple regression procedure for the determination of the equilibrium

* Corresponding author. Tel.: +55 313536 3402; fax: +55 31 34095700; e-mail address: leandroj.santos@ufv.br (L.J. Santos).

0040-4020/$ – see front matter © 2010 Elsevier Ltd. All rights reserved.
doi:10.1016/j.tet.2010.10.066

constant of complex absorbing mixtures in Zn-porphyrin/fullerene systems. Our protocol employs a computational approach rather than the usual graphical methods for treating spectrophotometric titration data; the software of choice was SQUAD (Stability Quotients from Absorbance Data).[22] This program is capable of calculating simultaneously, or individually, overall stability constants for any species formed in studied systems, as long as the species contributes to the total absorbance measured.[22] Early studies confirmed the ability of the program to evaluate the correctness of the equilibrium model proposed and the values of the refined equilibrium constants.[22] To the best of our knowledge, fullerene/porphyrin assembly coordination equilibrium data have been processed by only one computational (multiple regression) means.[17,20]

2. Results and discussion

2.1. Synthesis

The strategy explored for the preparation of the fullerene derivatives **6**, **7**, and **8** was based on a Bingel-type reaction (Scheme 1).[23,24]

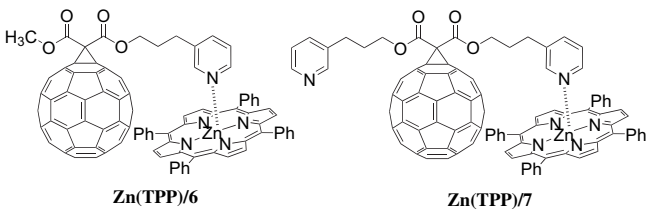

Fig. 1. Structures of the 1:1 supramolecular complexes investigated in the present study.

bridge signal was observed at 52 ppm. The molecular composition and the purity of the fullerene ligands **6** and **7** are also confirmed by ultra-high-resolution Fourier-transform mass spectrometry with electrospray ionization. Molecular masses of all isotopologue ions within the $[M+H]^+$ clusters agree well with calculated values.

2.2. Spectrophotometric titration

Zn-porphyrins are well-established, suitable spectroscopic probes for studying Lewis acid/base-type coordination equilibria in solution.

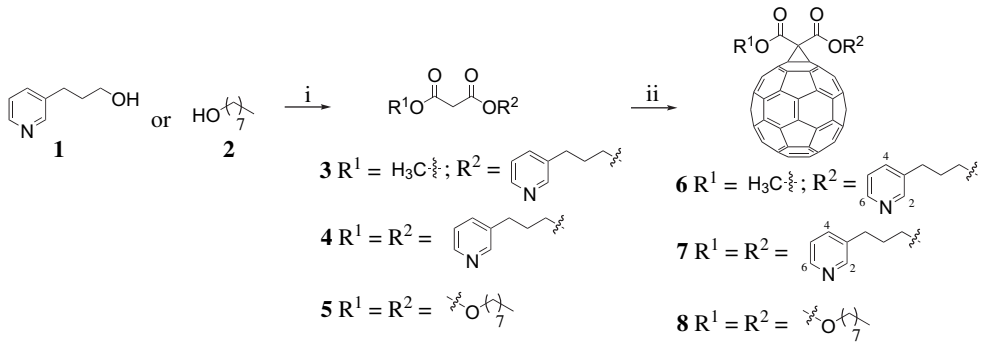

Scheme 1. Preparation of fullerene derivatives **6**, **7**, and **8**. Reagents and conditions: (i) methyl malonyl chloride or malonyl dichloride, pyridine, THF, room temperature, **3** (2 h, 83%), **4** (5 h, 57%), **5** (5 h, 74%); ii) C_{60}, I_2, DBU, toluene, room temperature, 8 h, **6** (50%), **7** (40%), **8** (50%).

The commercial alcohol **1** was esterified with commercial methyl malonyl chloride or malonyl dichloride in pyridine/THF mixtures at room temperature to yield the malonates **3** or **4** in 83% or 57% yield, respectively. The reaction of C_{60} with **3** or **4**, I_2, and DBU in toluene at room temperature afforded mono-adducts **6** or **7** in 50% or 40% yield, respectively, after purification by column chromatography. The advantages of this synthetic method for the preparation of the new compounds **6** and **7** include the overall simplicity of the procedure and the ready availability of the starting materials; additionally, this methodology can be easily adapted for the synthesis of other functionalized fullerenes. The fullerene derivative **8**, which does not contain the pyridyl moiety, was obtained from 1-octanol via the same method used for the synthesis of **6** and **7** (Scheme 1).

The applicability of the resulting compounds in supramolecular chemistry is demonstrated below by their ability to engage in coordination-type assemblies with metal complexes in solution, e.g., fullerene/Zn-porphyrin adducts. As a proof of concept, a study was undertaken to evaluate the ability of these new ligands **6** and **7** to assemble with Zn(TPP), to yield the corresponding Zn-porphyrin/fullerenes (Fig. 1) via the coordination route.

The structure and purity of the compounds were confirmed by ^1H and ^{13}C NMR spectroscopy (the spectra of the fullerene ligands are available in the Supplementary data). The ^{13}C NMR spectra of the fullerene ligands showed the characteristic signal[25] of the sp^3-hybridized fullerene C-atoms in the cyclopropane ring at ca. 71 ppm and the signals between 139 and 145 ppm corresponding to the sp^2-hybridized carbons of the fullerene sphere. The methano

The Zn(TPP) UV–vis absorption spectrum in hydrocarbon solvents, such as toluene, is characterized by a strong Soret band (λ=423 nm, in toluene) and a weaker Q band (λ=550 nm, in toluene). In the presence of a nitrogen/ligand (L), a rapid Lewis acid/base equilibrium is established to yield the Zn(TPP)/L adduct (ML) (where M=Zn(TPP) and L=ligand), according to Eq. 1. The formation of the ML species is accompanied by a red-shift of the Soret and the Q bands in a concentration-dependent manner, which makes UV–vis spectroscopy a suitable technique to study such systems. The spectrophotometric data are often analyzed graphically by a classical Benesi–Hildebrand (B–H) plot, given that there are only two absorbing species in equilibrium (i.e., M/ML or L/ML). Although this is usually the case for simple pyridine derivatives, fullerene-functionalized pyridines (such as **6** and **7**) absorb in the UV–vis region, which yields three chromophores (M, L, and ML) simultaneously in equilibrium and precludes the direct use of the B–H-type of analysis. To overcome these analytical issues, previous studies[8,10,17,18,20,21,26] on the coordination equilibrium of fullerenes to metalloporphyrins in solution are based on fluorescence data instead of UV–vis spectroscopy, as the fluorescence of Zn(TPP) (M) is quenched in a concentration-dependent manner by a non-fluorescent ligand (fullerene, L) to yield a non-fluorescent adduct (ML). We show here that the supramolecular assembly of functionalized fullerenes and Zn porphyrins may be conveniently measured by UV–vis spectrophotometry even in the case of strongly absorbing fullerene species, given that the data are appropriately treated by a multiwavelength spectrophotometric titration processing program, such as SQUAD. It is worth noting that, as

opposed to spectrofluorometers, UV–vis spectrophotometers require only simple setup and are widely available in most organic/inorganic laboratories.

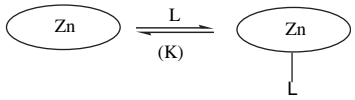

(1)

A set of UV–vis spectrophotometric titrations was designed to study the ability of **6** and **7** to assemble coordinatively with Zn(TPP) in solution. Titrations with unsubstituted pyridine (Py), with fullerene-free substituted pyridines **3** and **4**, and with pyridine-free fullerene **8** were carried out as controls for the supramolecular assemblies of Zn(TPP)/**6** and Zn(TPP)/**7**. The spectrophotometric titrations of Zn(TPP) with the fullerene ligands **6** and **7** (Scheme 1) were accompanied by the expected red-shifts of the Zn(TPP) Soret and Q bands (Fig. 2a and b). However, the titrations did not show the characteristic well-defined isosbestic points (Fig. 2a and b) usually associated with the two-species M/ML equilibrium of Zn(TPP)/simple Py ligand systems because **6** and **7** themselves absorb strongly in the titration region. As previously mentioned, fullerene-functionalized pyridines absorb in the UV–vis region, which results in the presence of three chromophores (i.e., M, L, and ML) simultaneously in equilibrium. The UV–vis spectra of the spectrophotometric titration of Zn(TPP) with **8** (Fig. 2c), which contains only the fullerene chromophore but no Py moiety, are superimposable on the sum of the absorbances of the two individual species. This observation shows that (i) the interaction between the fullerene moiety and Zn(TPP) is negligible (if present at all), (ii) the assembly of Zn(TPP)/**6**, and Zn(TPP)/**7** takes place through and is primarily controlled by the coordination of the Py moiety, and (iii) fullerene-free compounds **3** and **4** (along with Py itself) represent suitable models for **6** and **7**.

The spectrophotometric titrations of Zn(TPP) with Py, **3**, and **4**, which do not absorb in the Zn(TPP) Soret and Q band regions, showed well-defined isosbestic points along with the expected spectral red-shift (Fig. S1–3 in the Supplementary data). Spectrophotometric data for these titrations were evaluated both by the classic graphical B–H method and a computational approach using the software SQUAD (see below). These analyses reveal the stoichiometry and the formation constants[27] (K) of the Zn-porphyrin–ligand complex in solution.

$$\log\left(\frac{A-A_0}{A_\infty-A}\right) = n\log[\mathrm{L}] + \log(\mathrm{K}) \qquad (2)$$

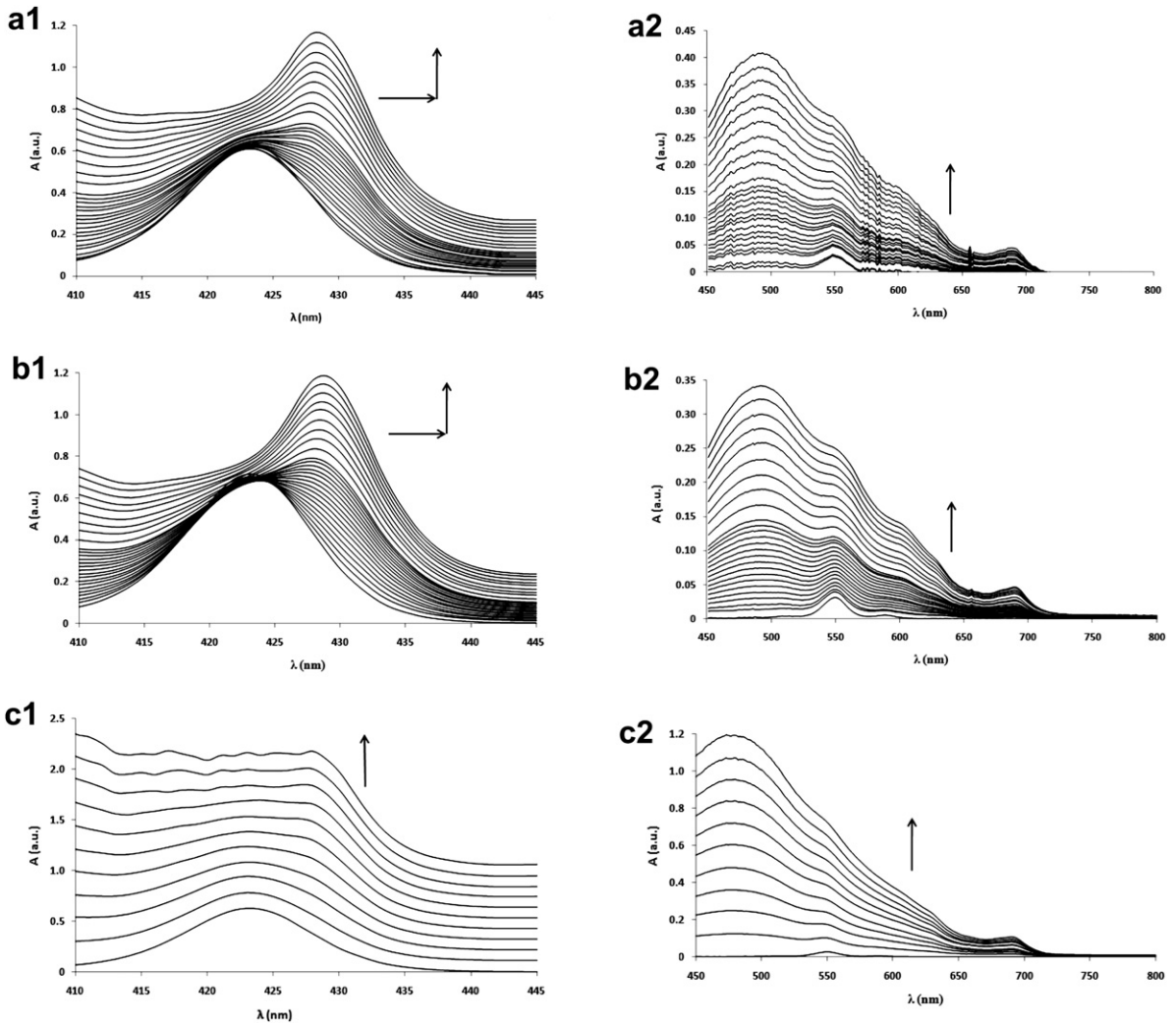

Fig. 2. Spectral shifts for the change of absorbance in the spectrophotometric titration titration in toluene. (*a*1–*a*2) Zn(TPP)/**6**; (*b*1–*b*2) Zn(TPP)/**7**; and (*c*1–*c*2) Zn(TPP)/**8**. Conditions: 7.93×10^{-6} mol L^{-1}<[ligands]<2.73×10^{-3} mol L^{-1}; 1.23×10^{-6} mol L^{-1}<[Zn(TPP)]<1.83×10^{-6} mol L^{-1}.

The B–H method consists of the analysis of the changes in absorbance (at a single wavelength) that accompany the change in concentration of L at a fixed Zn(TPP) concentration, according to Eq. 2, where A_0 is the initial absorbance of Zn(TPP) at a given wavelength in the absence of L; A_∞ is the absorbance in the end of the titration once A becomes independent of the concentration of L and corresponds to the species Zn(TPP)/L_n; A is the absorbance of the titrated solution at any intermediate concentration between those associated with A_0 and A_∞; K is the formation constant; and n is the number of ligands (L) in the complex.

Table 1 shows the equilibrium parameters obtained for the spectrophotometric titration of Zn(TPP) with Py, **3**, and **4** by the B–H method at two different wavelengths (λ=423 nm or 429 nm). The experimental data relative to the slope (n) in Eq. 2 (Table 1) indicate that the species M, L, and ML in the Zn(TPP)/Py, Zn(TPP)/**3**, and Zn(TPP)/**4** systems coexist in solution in an equilibrium state governed by the formation constant K. However, the B–H analysis at different wavelengths (λ=423 nm or 429 nm) returns K values of up to one order of magnitude apart in the same titration. This wavelength-dependence on the quantitative description of the equilibrium constant, associated with the fact that the B–H analysis is limited to ligands whose absorbance do not overlap considerably with Zn(TPP), precluded the appropriate analysis of the Zn(TPP) titration with **6** and **7** by the B–H method and prompted us to investigate the alternate multiwavelength computational approach provided by SQUAD.

Table 1
Parameters supplied by the B–H method in analyzing the spectrophotometric titration of Zn(TPP) with Py, **3**, and **4**

System	λ=423 nm				λ=429 nm			
	log K	K (M^{-1})	N	R^2	log K	K (M^{-1})	**n**	R^2
Zn(TPP)/Py	3.38	2.40×10^3	0.9	0.9931	4.46	2.88×10^4	1.2	0.9995
Zn(TPP)/**3**	3.65	4.47×10^3	1.0	0.9931	4.14	1.38×10^4	1.1	0.9992
Zn(TPP)/**4**	4.16	1.46×10^4	1.1	0.9983	4.37	2.34×10^4	1.1	0.9991

R^2=coefficient of linearity.

A systematic analysis of the spectrophotometric titration data of Zn(TPP) with the various ligands Py, **3**, **4**, **6**, **7**, or **8** was undertaken using the software SQUAD, a well-established Fortran-based data processing software[22] capable of executing calculations of the best values of the formation constants for a proposed equilibrium model. This software uses a nonlinear least squares approach to simultaneously fit absorption data at multiple wavelengths for solutions of varying ligand concentration.

The formation constants and the statistical parameters generated by SQUAD for the proposed M/L/ML equilibrium model for the titrations of Zn(TPP) with the various ligands are summarized in Table 2. In all calculations using SQUAD, the input file contained data of 25 spectra per titration; a total of 50 wavelengths per spectrum (i.e., 1250 data points per titration) were simultaneously examined in the region of the Soret band of Zn(TPP) and the resulting Zn(TPP)/L species. When the analyses of the Zn(TPP)/Py, Zn(TPP)/**6**, and Zn(TPP)/**7** were carried out in the visible region of the spectrum (516–618 nm), the formation constants (K) calculated were comparable to those obtained in the Soret region (Table 2). This result indicates that the absorption band of fullerenes near the Soret band of Zn(TPP) does not interfere with the analysis of this spectral region by SQUAD. Convergence was not achieved for any equilibrium model in the Zn(TPP) titration with **8**, which is consistent with the lack of any significant interaction between the pyridine-free fullerene and Zn(TPP).

Table 2
Parameters supplied by the SQUAD program for the spectrophotometric titration of Zn(TPP) with Py, **3**, **4**, **6**, and **7**

System	log K	K (M^{-1})	σ_{data}	Σ (obsd−calcd)^2
Zn(TPP)/Py	3.686±0.003 (3.62±0.01)[a]	4.853×10^3	0.004	0.01
Zn(TPP)/**3**	3.646±0.002	4.426×10^3	0.003	0.009
Zn(TPP)/**4**	3.930±0.001	8.511×10^3	0.003	0.008
Zn(TPP)/**6**	3.683±0.007 (3.53±0.02)[a]	4.819×10^3	0.006	0.03
Zn(TPP)/**7**	3.794±0.008 (3.71±0.02)[a]	6.223×10^3	0.002	0.004

[a] Analyses carried out independently in the visible region of the spectrum (516–618 nm) of Zn(TPP) to yield Zn(TPP)/L species.

Good reproducibility in the equilibrium parameters that govern the solution assembly of Zn(TPP) with Py, **3**, **4**, **6**, and **7** was obtained by the computational approach; the formation constants varied by ~5% with a second titration (replicate). This result demonstrates the accuracy of both the experimental methodology and the data processing and calculations by SQUAD. The formation constants found (Table 2) are in an excellent agreement with those previously reported for the interaction of Zn(TPP) with other related fullerenes functionalized with *N*-containing moieties, for which different methods of analysis of the experimental data were used.[13,14,16,18,19,20]

For the titration of Zn(TPP) by **7** an attempt to fit the experimental data to a model including a 2:1 porphyrin/fullerene complex was unsuccessful: no binding constant could be calculated from the UV titration data as the chemical model including this M_2L species precluded the minimization and convergence process of the regression spectral analysis. This is likely ascribed to either the 2:1 complex not being formed at all or because the conditions for its formation are not accessible within the concentration limits of the spectrophotometric titrations. It is unreasonable to assume that only one pyridine unit of **7** coordinates to the zinc porphyrin, but considering that Zn(TPP) forms exclusively pentacoordinate stable complexes at room temperature,[28] the two pyridine-moiety nitrogen atoms of **7** cannot bind simultaneously to the Zn porphyrin, as this would result in a hexacoordinated complex. Therefore, a dynamic, intramolecular equilibrium is likely to be established for the 'two-point'-bonded 1:1 Zn(TPP)/**7** complex as shown in Scheme 2. It is worth noting that a 'two-point' binding motif has been suggested for systems as such by Li and coworkers.[29]

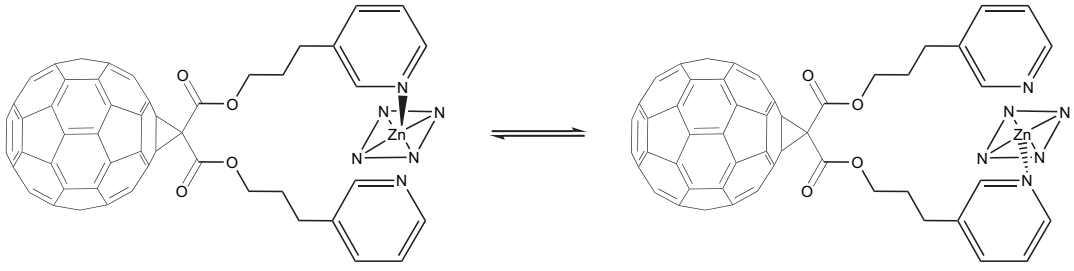

Scheme 2. Dynamic process for the proposed 'two-point' binding mode for the complexes of **7** with Zn(TPP) guest.

SQUAD calculates both the formation constants and, if requested, the molar absorptivity of the species in equilibrium. A significant improvement of 26–65% in the statistical parameters was achieved by fixing the molar absorptivity of L to the experimental values and letting SQUAD calculate the molar absortivities of both M and ML (as opposed to fixing both L and M). The agreement between the molar absorptivity of Zn(TPP) determined experimentally and that calculated by SQUAD in each titration model directly from the titration data (Fig. 3) represents another means to validate the calculations performed by SQUAD. Once the constants for the modeled chemical equilibrium have been determined, the emulation of the experimental absorption spectra, including the molar absorptivity coefficients at each wavelength, becomes possible via data processing using SQUAD (Fig. 3). It is also worth noting that the access to the molar absorptivity of all of the species involved in the solution equilibrium is not granted by the B–H method. Fig. 3 shows the molar absorptivity spectra of all of the

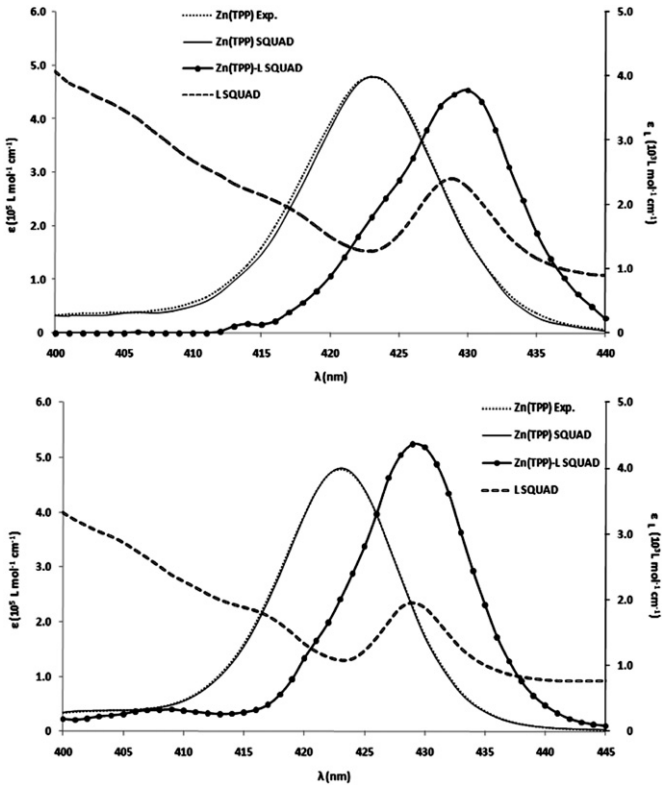

Fig. 3. Molar absorptivity of the species calculated by SQUAD (M, ML and L) or experimentally determined (M). Titration in toluene of Zn(TPP) with either **6** (top) or **7** (bottom).

chromophore species present in the Zn(TPP) titration with **6** and **7**, including those of the Zn(TPP)/**6** and Zn(TPP)/**7** assemblies. The spectra calculated by SQUAD for all Zn(TPP)/L species (L=Py, **3**, **4**, **6**, and **7**) in equilibrium were very similar to each other, which is consistent with Zn(TPP) being the chromophore of higher molar absorptivity in theses species; the molar absorptivity of the fullerenes **6** and **7** calculated by SQUAD agrees with that measured experimentally and is one order of magnitude lower than that of Zn (TPP). The similarity of the molar absorptivity of the Zn(TPP)/L species (L=Py, **3**, **4**, **6**, and **7**) is also consistent with the Zn(TPP)/L binding motif in all ML species being essentially the same (i.e., coordination via an unencumbered pyridine moiety).

The formation of the supramolecular systems Zn(TPP)/**6** and Zn (TPP)/**7** is also supported by ^{1}H nuclear magnetic resonance (NMR) and electrochemical data.

2.3. NMR titration

The complexation between Zn(TPP) and the fullerene ligands **6** and **7** was also demonstrated by NMR titration. Fig. 4 shows the ^{1}H NMR spectral data for Zn(TPP) at various concentrations of **6**. A significant shielding of the protons of the ligand was observed upon coordination to Zn(TPP). The 2,6-pyridine protons, 4-pyridine proton and 5-pyridine proton showed up as broad singlets shifted upfield as compared to that of unbound ligand **6**. Upon addition of 1 equiv of ligand **6** (Fig. 4c), the 2,6-pyridine protons experienced a shielding of nearly 4.5 ppm due to the complexation; the 4-pyridine proton and 5-pyridine proton located at 7.27 and 7.56 ppm in the unbound ligand were shifted to 6.54 and 5.92 ppm, respectively; and the CH_2O protons experienced a shielding of 0.5 ppm. The greater shift observed for the pyridine protons relative to other protons of **6** can be rationalized by the greater proximity of the axially coordinated Py moieties to the porphyrin plane, which results in a greater shielding by the porphyrin ring π-currents.[17] No peaks for unbound ligand **6** were observed under these conditions. With increasing concentration of ligand in the mixture, the spectral pattern approximated that of the free ligand **6**, as the

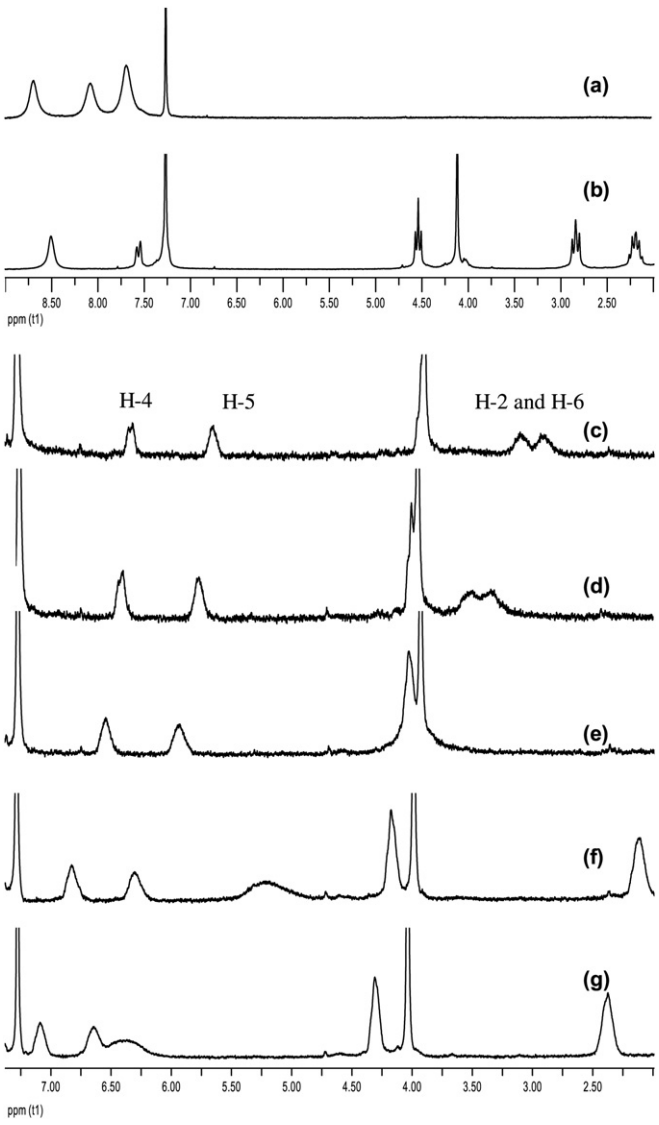

Fig. 4. ^{1}H NMR spectrum of (a) Zn(TPP); (b) **6**; (c) Zn(TPP)/**6** (1:0.5); (d) Zn(TPP)/**6** (1:0.75); (e) Zn(TPP)/**6** (1:1); (f) Zn(TPP)/**6** (1:1.5); (g) Zn(TPP)/**6** (1:2.5) in $CDCl_3$.

M/L/ML rapid equilibrium in Zn-porphyrin/nitrogen-base systems is much faster than the NMR time-scale.[30]

The ^{1}H NMR titration of Zn(TPP) by ligand **7** presented the same pattern as of that of **6**, up to the 1:1 M ratio of Zn(TPP) and **7** (Fig. S5 in the Supplementary data). With increasing concentration of **7** in the mixture, there happens an unfolding of pyridine signs, which may originate from the stabilization of the non-symmetric system suggested by the dynamic equilibrium illustrated in Scheme 2.

2.4. Electrochemical studies

The investigation of the electrochemical properties of the fullerene ligands and their corresponding assemblies with Zn(TPP) was done by cyclic voltammetry. The study was aimed at gathering information on the redox potentials of the compounds and the possible electronic interaction between the donor (Zn(TPP)) and acceptor (fullerene in ligands **6** and **7**) moieties of the Zn(TPP)/**6** and Zn(TPP)/**7** assemblies in solution.

Fig. 5 shows the cyclic voltammograms of C_{60}, **6**, and **7** recorded under the same conditions for comparison purposes, while Table 3 lists the first three $E_{1/2}$ values associated with these species. The cyclic voltammogram of **6** and **7** is characterized by a cathodic shift of these potentials relative to the corresponding processes in C_{60}. An irreversible anodic peak at −0.34 V and −0.19 V for **6** and **7**, respectively, was also observed.

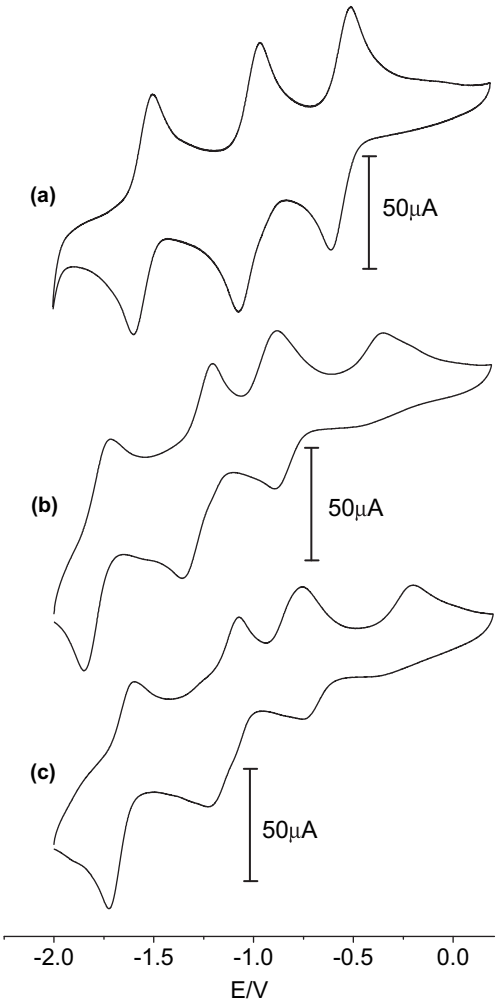

Fig. 5. Cyclic voltammogram of (a) C_{60}, (b) **6** and (c) **7** in 0.1 mol L^{-1} of Bu_4NBF_4 *o*-dichlorobenzene/*N*,*N*-dimethylformamide (1:1). Scan rate: 50 mV s^{-1}.

Table 3
$E_{1/2}$ versus Ag/$AgNO_3$ for C_{60} and fullerene ligands **6** and **7**

Compounds	$E_{1/2}$ versus Ag/$AgNO_3$		
	E_1/V	E_2/V	E_3/V
C_{60}	−1.54	−1.00	−0.55
6	−1.77	−1.27	−0.87
7	−1.65	−1.14	−0.75

Fig. 6 shows the cyclic voltammograms of Zn(TPP) and the Zn(TPP)/**6** and Zn(TPP)/**7** assemblies at 50 mV s^{-1}. For Zn(TPP) (Fig. 6a), the presence of two oxido-reduction processes can be ascribed to the formation of a π-cation radical (0.57 V vs Ag/$AgNO_3$) and a dication radical (0.88 V vs Ag/$AgNO_3$).[15] Zn(TPP)/**6** (Fig. 6a) and Zn(TPP)/**7** (Fig. 6c) have an oxido-reduction process at 0.58 V and 0.62 V, respectively, in which the potential values of the peak-to-peak (anodic and cathodic) separation and the cathodic-to-anodic peak current ratio indicated an electrochemically quasi-reversible behavior. The coordination of **6** with Zn(TPP) (Fig. 6b) is accompanied by a significant positive shift of the redox potentials, indicating the presence of interactions between the porphyrin π-system (donor) and the fullerene core (acceptor).

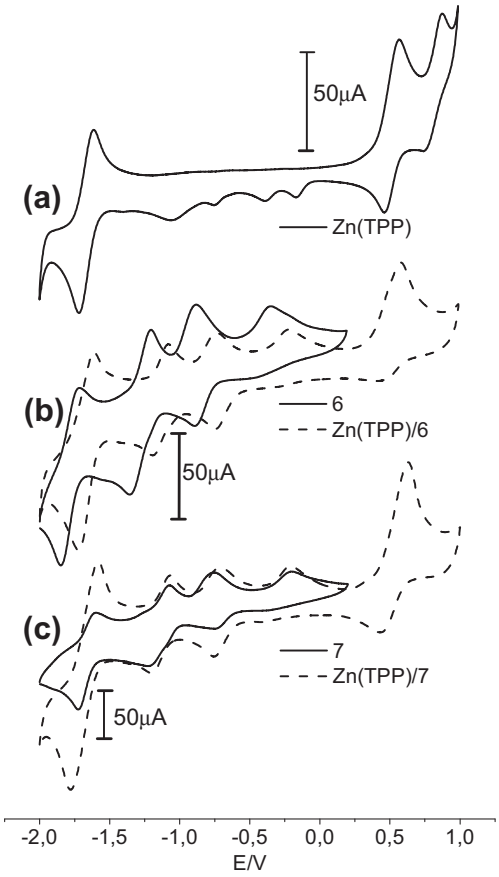

Fig. 6. Cyclic voltammogram of (a) Zn(TPP) and (b and c) fullerene-free ligands and complexes. Scan rate: 50 mV s^{-1}.

Conversely, the coordination of **7** with Zn(TPP) did not result in any significant change in the redox potential of the C_{60} moiety. This result implies an absence of π–π charge transfer interactions between the porphyrin π-system and the fullerene core in the Zn(TPP)/**7** assembly (Fig. 6c), which suggests a rapid coordination equilibrium between the two pyridyl moieties of the fullerene derivative **7** and Zn(TPP) (Scheme 2). This results in low-to-nonexistent π–π charge

transfer interactions between the porphyrin π-system and **7** within the supramolecular complex Zn(TPP)/**7** (Scheme 2).

3. Conclusions

We have shown here that new fullerene ligands can be easily prepared following a Bingel-type cyclopropanation reaction, and we have demonstrated the applicability of these ligands in supramolecular chemistry by their coordinative assembly with a Zn-porphyrin. The coordination equilibrium was investigated by UV–vis and NMR titrations and by electrochemical means.

The formation constants relative to the axial coordination of Zn(TPP) with the new fullerene ligands were determined spectrophotometrically and conveniently calculated by using the program SQUAD. The analysis of multiwavelength data by SQUAD is often significantly more robust than examination of a single wavelength (B–H method) and was used here for the analysis of porphyrin/fullerene dyads for the first time. Additionally, SQUAD analysis allows the determination of the pure spectra of all of the species and intermediates in the equilibrium system. These results show that analyses of multiwavelength data are particularly promising for studying the nature, stoichiometry, and spectral properties of complex assemblies of fullerenes and metalloporphyrins in solution.

The formation constants for the interaction between Py, **3**, **4**, **6**, or **7** with Zn(TPP) are close to each other (Table 2), which indicates that the assembly of the adducts in solution is controlled primarily by the pyridine moiety and is little influenced by the fullerene in **6** and **7**. It is worth noting that in the absence of any synergistic effect between the porphyrin and the fullerene moiety, the relatively low values for the formation constants of Zn-porphyrin/*N*-heteroaromatic-functionalized fullerene dyads imply that the isolated supramolecular assemblies (ML) may not be of particular relevance as cellular sensitizers[31] given that once in solution, the equilibrium is shifted to the individual constituents M and L under biologically relevant conditions (i.e., at total stoichiometric concentrations lower than 10^{-5} mol L^{-1}, ML constitutes <10% of the M/L/ML mixture). Additionally, whereas the use of more concentrated solutions (>10^{-3} mol L^{-1}) may warrant the formation of the Zn(TPP)/fullerene adduct in considerable amount, at concentrated solutions other processes such as association between ground-state molecules, which gives rise to dimers and higher aggregates, and interactions between excited and ground-state of the molecules may take place and limit, thus, the use of these assemblies as photoactive materials.[32]

Additionally, the lack of significant steric hindrance between the two very bulky and sterically demanding moieties (i.e., the porphyrin and the fullerene moieties) in the dyads is granted by the flexibility of the malonate chains, which function as an appropriate pyridine-fullerene linker for the design of unencumbered porphyrin/fullerene assemblies. The easy access to malonate-functionalized fullerene derivatives via the Bingel-type chemistry as described here provides a convenient method for the preparation of other more elaborate fullerene-based ligands for the synthesis of tailored porphyrin-based donor/acceptor dyads.

4. Experimental

4.1. Materials and methods

Reagents and solvents were of reagent grade and used without further purification unless stated otherwise. Tetrahydrofuran (THF) was distilled over sodium benzophenone. C_{60} (99.5%) was obtained from M.E.R. Corporation. Preparation and characterization data of the malonates **3**, **4**, and **5** are described in the Supplementary data. NMR spectra were recorded in $CDCl_3$ on a Bruker Avance DPX-200 (200 MHz) spectrometer and referenced to either the residual $CDCl_3$ (δ 7.26) or tetramethyl silane (TMS) protons. Fourier-transform mass spectroscopy (FT-MS) was performed with an LTQ FT ULTRA (ThemoScientific-7 T-Germany) instrument with the TriVersa NanoMate system (Advion, USA) operating in the chip-based infusion mode and in the positive ion mode using a silicon-based integrated nanoelectrospray microchip. Column chromatography was carried out using silica gel 60, 70–230 mesh (Merck). UV–vis spectra (190–1100 nm) were recorded in a Hewlett–Packard 8453 diode-array spectrophotometer. Multiwavelength spectrophotometric data analyses were carried out on a Pentium IV computer using SQUAD software.[22]

4.2. General procedures for the synthesis of fullerene derivatives

To a solution of C_{60} (0.35 g, 0.48 mmol) in toluene (350 mL) were added iodine (0.18 g, 0.72 mmol), malonate **3**, **4**, or **5** (0.48 mmol), and diaza(1,3)bicyclo[5.4.0]undecane (DBU) (180 μL, 1.2 mmol). The reaction mixture was stirred for 8 h at room temperature, under nitrogen atmosphere, and then filtered. The solvent was removed under reduced pressure, and the residue was purified by column chromatography, eluting first with toluene (to remove unreacted C_{60}). The pure mono-adduct was isolated by eluting with 30% MeOH in EtOAc (for compounds **6** and **7**) or with 5% AcOEt in toluene (for compound **8**) to provide the fullerene derivatives **6**, **7** or **8** in 50%, 40% and 50% yield, respectively.

*4.2.1. Compound **6**.* IR (compression cell): ν 3022, 3002, 2951, 2853, 1540, 1428, 1740, 1231, 1186. ^{1}H NMR ($CDCl_3$): δ 2.20 (pseudo qn, 2H, CH_2CH_2O), 2.85 (t, 2H, J=7.2 Hz, CH_2Py), 4.13 (s, 3H, OCH_3), 4.55 (t, 2H, J=6.2 Hz, CH_2O), 7.27 (br s, 1H, *H*-Py), 7.58 (d, 1H, J=7.8 Hz, *H*-Py), 8.50–8.52 (m, 2H, *H*-Py). ^{13}C NMR (50 MHz, $CDCl_3$): δ 29.4, 30.0 ($2CH_2$), 52.0 (methano bridge), 54.2 (OCH_3), 66.3 (CH_2O), 71.5 ($2C_{60}$-sp^3), 123.7, 136.0, 136.1, 148.0, 150.0 (5*C*-Py), 139.0, 139.3, 141.1, 141.3, 142.0, 142.5, 143.5, 144.4, 144.8, 145.0, 145.1, 145.3, 145.4 (58*C*-fullerene), 163.6 (*C*=O), 164.1 (*C*=O). $C_{72}H_{13}NO_4$. UV–vis in toluene, λ_{max}, nm (log ε): 428 (3.38), 493 (3.16). Exact mass calculated for $[M+H]^+$ (M=956.08446). Found FT-MS ESI(+): m/z 956.09276.

*4.2.2. Compound **7**.* IR (compression cell): ν 3027, 2957, 2921, 2860, 1726, 1148, 1022. ^{1}H NMR ($CDCl_3$): δ 2.18 (pseudo qn, 4H, CH_2CH_2O), 2.82 (t, 4H, J=7.2 Hz, CH_2Py), 4.55 (t, 4H, J=6.2 Hz, CH_2O), 7.22–7.28 (m, 2H, *H*-Py), 7.54 (d, 2H, J=7.6 Hz, *H*-Py), 8.50 (br s, 4H, *H*-Py). ^{13}C NMR (50 MHz, $CDCl_3$): δ 29.5, 30.0 ($4CH_2$), 52.2 (methano bridge), 66.4 ($2CH_2O$), 71.6 ($2C_{60}$-sp^3), 123.8, 136.8, 147.9, 149.8 (10*C*-Py), 139.1, 141.2, 142.0, 142.3, 143.2, 144.0, 144.7, 144.8, 145.1, 145.2, 145.4 (58*C*-fullerene), 163.7 (2*C*=O). $C_{79}H_{20}N_2O_4$. UV–vis in toluene, λ_{max}, nm (log ε): 428 (3.30), 493 (3.07). Exact mass calculated for $[M+H]^+$ (M=1061.14231). Found FT-MS ESI(+): m/z 1061.15122.

*4.2.3. Compound **8**.* IR (compression cell): ν 2951, 2920, 2850, 1742, 1539, 1427, 1226, 1185. ^{1}H NMR ($CDCl_3$): δ 0.79–0.82 (m, 6H, CH_3), 1.22 (br s, 16H, $CH_3(CH_2)_4CH_2$), 1.53 (br s, 4H, $CH_2CH_2CH_2O$), 1.70–1.81 (m, 4H, CH_2CH_2O), 4.42 (t, 4H, J=6.6 Hz, CH_2O). ^{13}C NMR (50 MHz, $CDCl_3$): δ 14.3 ($2CH_3$), 22.8, 26.1, 28.7 ($8CH_3(CH_2)_4CH_2$), 29.4 ($2CH_2CH_2CH_2O$), 32.0 ($2CH_2CH_2O$), 52.5 (methano bridge), 67.6 ($2CH_2O$), 71.8 ($2C_{60}$-sp^3), 139.1, 141.0, 142.0, 142.3, 143.1, 144.0, 144.7, 144.8, 145.0, 145.3, 145.4, 145.5 (58*C*-fullerene), 163.8 (2*C*=O). $C_{79}H_{34}O_4$ (1046.00 g mol^{-1}). UV–vis in toluene, λ_{max}, nm (log ε): 428 (4.39), 476 (4.20).

4.2.4. Zn(TPP). Zn(TPP) was prepared by metalation of H_2TPP (Sigma–Aldrich) with $Zn(OAc)_2 \cdot 2H_2O$ using the standard chloroform/methanol method.[33] Briefly, to a refluxing solution of H_2TPP (83.27 mg, 0.135 mmol) in CH_2Cl_2 (20 mL) was added $Zn(OAc)_2 \cdot 2H_2O$ (147.76 mg, 0.67 mmol) in MeOH (5 mL). The resulting solution was kept under reflux for 1 h. After this time, the solvent was evaporated,

and the residue was purified by column chromatography on neutral alumina. The column was eluted with CH_2Cl_2. The purple fraction corresponding to Zn(TPP) was collected and evaporated to dryness. The resulting purple solid was kept over P_2O_5 under vacuum in a desiccator. UV–vis in toluene, λ_{max}, nm (log ε): 423 (5.68), 550 (4.40). ^{1}H NMR ($CDCl_3$, TMS): δ 7.77–7.79 (m; 12H; *m*- and *p*-HPh), 8.22–8.24 (m; 8H; *o*-H Ph), 8.95–8.96 (m; 8H; β-pyrrole).

4.3. Spectrophotometric titration

Spectrophotometric titrations were performed in a borosilicate glass cuvette tightly capped with a Teflon-coated silicon septum using a 25.0±0.1 °C thermostatized cell-holder. All stock and working solutions were kept in the dark fully wrapped with aluminum foil. Additionally, the titration was carried out with minimal ambient light exposure, and the spectrophotometer shutter was kept closed in between measurements. The initial concentration of the toluene solutions of Zn(TPP) in the cuvette was determined spectrophotometrically; typical values were from $1.23–1.83\times10^{-6}$ mol L^{-1}. Aliquots of the toluene stock solutions of the titrating ligands (Py, **3**, **4**, **6**, **7**, or **8**) were added consecutively to the cuvette through the cuvette silicon septum with Hamilton microsyringes; immediately prior to recording the UV–vis spectrum, the system was magnetically stirred for 1 min at 25.0±0.1 °C to allow for thermal and chemical equilibration after the addition of each ligand aliquot. The total concentration of the ligands in the cuvette ranged from 7.93×10^{-6} mol L^{-1} to 2.73×10^{-3} mol L^{-1}. The end of the titration was determined when UV–vis spectral variations ceased. Dilution effects along the titration were accounted for when calculating the total concentration of Zn (TPP) and ligand at each titration point. The mathematical treatment of the absorbance versus concentration data was carried out either graphically (via Benesi–Hildebrand plots) or computationally[22] (using the software SQUAD).

4.4. Electrochemical experiments

The electrochemical experiments were carried out using an AUTOLAB (PGSTAT 302) ECOChemie potentiostat–galvanostat. The electrochemical experiments were carried out in a typical three-electrode cell; a vitreous carbon disk electrode ($A=2.8\times10^{-2}$ cm^2) was used as the working electrode, a platinum wire was used as the counter electrode, and a Ag/0.1 M $AgNO_3$ served as the reference electrode in acetonitrile. The electrochemical profile was recorded in 1:1 *o*-dichlorobenzene/*N*,*N*-dimethylformamide solutions of Zn(TPP) (0.002 mol L^{-1}), fullerene or fullerene-free ligand (0.002 mol L^{-1}), and tetrabutylammonium tetrafluoroborate (Bu_4NBF_4, 0.1 mol L^{-1}) at room temperature under nitrogen atmosphere.

4.5. NMR titration

The coordination of ligand **6** and **7** to Zn(TPP) was monitored spectroscopically by ^{1}H NMR. To a $CDCl_3$ solution of Zn(TPP) (6.50 mmol L^{-1}) were added appropriate amounts of **6** directly into the NMR tube to yield total concentrations of **6** within the 2.95–10.80 mmol L^{-1} range; upon each addition the corresponding spectrum was recorded. A analogous titration was carried out using **7** instead of **6** (data are given in the Supplementary data).

Acknowledgements

Financial support from The Brazilian Research Council (CNPq) and Fundação de Amparo à Pesquisa do Estado de Minas Gerais (FAPEMIG) is gratefully acknowledged. We also thank Laboratório ThoMSon de Espectrometria de Massas (Universidade Estadual de Campinas, SP-Brazil) for the mass spectrometric analyses.

Supplementary data

Synthetic details of the malonates **3**, **4**, and **5**. Spectral shifts, molar absorptivity of species calculated by SQUAD (M and ML) or experimentally determined (M) and B–H plot for change of absorbance in the systems Zn(TPP)/Py, Zn(TPP)/**3**, and Zn(TPP)/**4**. ^{1}H NMR spectra of the titration of ZnTPP by ligand **7**. ^{1}H and ^{13}C NMR spectra of the new fullerene derivatives **6**, **7**, and **8**. Supplementary data associated with this article can be found in online version at doi:10.1016/j.tet.2010.10.066. These data include MOL files and InChIKeys of the most important compounds described in this article.

References and notes

1. Clifford, J. N.; Accorsi, G.; Cardinali, F.; Nierengarten, J.-F.; Armaroli, N. *C. R. Chim.* **2006**, *9*, 1005.
2. (a) Imahori, H. *Org. Biomol. Chem.* **2004**, *2*, 1425; (b) Ito, O.; Yamanaka, K.-I. *Bull. Chem. Soc. Jpn.* **2009**, *82*, 316.
3. Marczak, R.; Sgobba, V.; Kutner, W.; Gadde, S.; D'Souza, F.; Guldi, D. M. *Langmuir* **2007**, *23*, 1917.
4. Guldi, D. M. *Chem. Soc. Rev.* **2002**, *31*, 22.
5. Liddel, P. A.; Sumida, J. P.; Macpherson, A. N.; Noss, L.; Seely, G. R.; Clark, K. N.; Moore, A. L.; Moore, T. A.; Gust, D. *Photochem. Photobiol.* **1994**, *60*, 537.
6. (a) Fazio, M. A.; Lee, O. P.; Schuster, D. I. *Org. Lett.* **2008**, *10*, 4979; (b) Iehl, J.; Osinska, I.; Louis, R.; Holler, M.; Nierengarten, J.-F. *Tetrahedron Lett.* **2009**, *50*, 2245; (c) Urbani, M.; Nierengarten, J.-F. *Tetrahedron Lett.* **2007**, *48*, 8111; (d) Schuster, D. I.; Li, K.; Guldi, D. M.; Palkar, A.; Echegoyen, L.; Stanisky, C.; Cross, R. J.; Niemi, M.; Tkachenko, N. V.; Lemmetyinen, H. *J. Am. Chem. Soc.* **2007**, *129*, 15973; (e) Fukuzumi, S.; Ohkubo, K.; Imahori, H.; Shao, J.; Ou, Z.; Zheng, G.; Chen, Y.; Pandey, R. K.; Fujitsuka, M.; Ito, O.; Kadish, K. M. *J. Am. Chem. Soc.* **2001**, *123*, 10676.
7. Fukuzumi, S.; Kojima, T. *J. Mater. Chem.* **2008**, *18*, 1427.
8. D'Souza, F.; Smith, P. M.; Rogers, L.; Zandler, M. E.; Islam, D.-M. S.; Araki, Y.; Ito, O. *Inorg. Chem.* **2006**, *45*, 5057.
9. Tat, F. T.; Zhou, Z.; MacMahon, S.; Song, F.; Rheingold, A. L.; Echegoyen, L.; Schuster, D. I.; Wilson, S. R. *J. Org. Chem.* **2004**, *69*, 4602.
10. D'Souza, F.; Zandler, M. E.; Gadde, S.; McCarty, A. L.; Karr, P. A.; El-Khouly, M. E.; Araki, Y.; Ito, O. *J. Phys. Chem. B* **2005**, *109*, 10107.
11. Yin, G.; Xu, D.; Xu, Z. *Chem. Phys. Lett.* **2002**, *365*, 232.
12. Uyar, Z.; Satake, A.; Kobuke, Y.; Hirota, S. *Tetrahedron Lett.* **2008**, *49*, 5484.
13. D'Souza, F.; Deviprasad, G. R.; Rahman, M. S.; Choi, J.-P. *Inorg. Chem.* **1999**, *38*, 2157.
14. D'Souza, F.; Deviprasad, G. R.; Zandler, M. E.; El-Khouly, M. E.; Fujitsuka, M.; Ito, O. *J. Phys. Chem. A* **2003**, *107*, 4801.
15. Deye, J. R.; Shiveley, A. N.; Goins, S. M.; Rizzo, L.; Oehrle, S. A.; Walters, K. A. *Inorg. Chem.* **2008**, *47*, 23.
16. Wu, Z.-Q.; Li, C.-Z.; Feng, D.-J.; Jiang, X.-K.; Li, Z.-T. *Tetrahedron* **2006**, *62*, 11054.
17. Trabolsi, A.; Urbani, M.; Delgado, J. L.; Ajamaa, F.; Elhabiri, M.; Solladié, N.; Nierengarten, J.-F.; Albrecht-Gary, A.-M. *New J. Chem.* **2008**, *32*, 159.
18. Armaroli, N.; Diederich, F.; Echegoyen, L.; Habicher, T.; Flamigni, L.; Marconi, G.; Nierengarten, J. F. *New J. Chem.* **1999**, *23*, 77.
19. (a) D'Souza, F.; Smith, P. M.; Gadde, S.; McCarty, A. L.; Kullman, M. J.; Zandler, M. E.; Itou, M.; Araki, Y.; Ito, O. *J. Phys. Chem. B* **2004**, *108*, 11333; (b) D'Souza, F.; Deviprada, G. R.; El-Khouly, M. E.; Fujitsuka, M.; Ito, O. *J. Am. Chem. Soc.* **2001**, *123*, 5277; (c) D'Souza, F.; Deviprada, G. R.; El-Khouly, M. E.; Fujitsuka, M.; Ito, O.; Klykov, A.; VanStipdonk, M.; Perera, A. *J. Phys. Chem. A* **2002**, *106*, 3243; (d) Wilson, S. R.; MacMahon, S.; Tat, F. T.; Jarowski, P. D.; Schuster, D. I. *Chem. Commun.* **2003**, 226.
20. Trabolsi, A.; Elhabiri, M.; Urbani, M.; de la Cruz, J. L. D.; Ajamaa, F.; Solladié, N.; Albrecht-Gary, A.-M.; Nierengarte, J.-F. *Chem. Commun.* **2005**, 5736.
21. Hauke, F.; Swartz, A.; Guldi, D. M.; Hirsch, A. *J. Mater. Chem.* **2002**, 2088.
22. Leggett, D. J.; Kelly, S. L.; Shiue, L. R.; Wu, Y. T.; Chang, D.; Kadish, K. M. *Talanta* **1983**, *30*, 579.
23. Bingel, C. *Chem. Ber.* **1993**, *126*, 1957.
24. Nierengarten, J.-F.; Habicher, T.; Kessinger, R.; Cardullo, F.; Diederich, F. *Helv. Chim. Acta* **1997**, *80*, 2238.
25. Diederich, F.; Isaacs, L.; Philp, D. *Chem. Soc. Rev.* **1994**, 243.
26. Xiang, X.; Wei, X.-W.; Zhang, X.-M.; Wang, H.-L.; Wei, X.-L.; Hu, J.-P.; Yin, G.; Xu, Z. *Inorg. Chem. Commun.* **2006**, *9*, 452.
27. Benesi, H. A.; Hildebrand, J. H. *J. Am. Chem. Soc.* **1949**, *71*, 2703.
28. Smith, K. M. *Porphyrins and Metalloporphyrins*; Elsevier: Amsterdam, 1975.
29. Li, C. Z.; Zhu, J.; Wu, Z. Q.; Hou, J. L.; Li, C.; Shao, X. B.; Jiang, X. K.; Li, Z. T.; Gao, X.; Wang, Q. R. *Tetrahedron* **2006**, *62*, 6973.
30. Kirskey, C. H.; Hambright, P.; Storm, C. B. *Inorg. Chem.* **1969**, *8*, 2141.
31. (a) dos Santos, L. J.; Alves, R. B.; de Freitas, R. P.; Nierengarten, J.-F.; Magalhães, L. E. F.; Krambrock, K.; Pinheiro, M. V. B. *J. Photochem. Photobiol., A* **2008**, *200*, 277; (b) Yamakoshi, Y.; Umezawa, N.; Ryu, A.; Arakane, K.; Miyata, N.; Goda, Y.; Masumizu, T.; Nagano, T. *J. Am. Chem. Soc.* **2003**, *125*, 12803; (c) Wang, S.; Gao, R.; Zhou, F.; Selke, M. *J. Mater. Chem.* **2004**, *14*, 487.
32. (a) Zinimermanc, A. A.; Orlando, J. R.; Gianni, M. H. *J. Org. Chem.* **1969**, *34*, 73; (b) Mochalov, I. A.; Lapshin, A. N.; Nadtochenki, V. A.; Smirnov, V. A.; Goldshleger, N. F. *Russ. Chem. Bull.* **2006**, *55*, 1598.
33. (a) Wijesekera, T. P.; Dolphin, D. A. In *Metalloporphyrins in Catalytic Oxidations*; Sheldon, R. A., Ed.; Marcel Dekker: New York, NY, 1994; pp 193–239; (b) Rebouças, J. S.; de Carvalho, M. E. M. D.; Idemori, Y. M. *J. Porphyrins Phthalocyanines* **2002**, *6*, 50.